ADVANCED MATERIALS

5 was prepared from benzoyl chloride and purified by column chromatography (SiO_2, 10:1 hexane/ethyl acetate) to afford 78 mg (40 %) of **5** as a yellow solid. Mp = 70–73 °C; ^{1}H NMR ($CDCl_3$): δ 2.29 (s, 3H, C*H*$_3$), 7.11 (s, 1H, thienyl-C*H*), 7.29 (m, 1H, ar C*H*), 7.36 (m, 4H, ar C*H*), 7.42 (m, 2H, ar C*H*), 7.53 (m, 1H, ar C*H*), 7.73 (m, 2H, arC*H*); MS (CI): 453 (M^+).

6 was prepared from 4-methoxybenzoyl chloride and purified by column chromatography (SiO_2, hexane/ethyl acetate 5:1) and recrystallization from hexane to afford 87 mg (82 %) of **6** as a yellow solid. Mp = 87–89 °C; ^{1}H NMR ($CDCl_3$): δ 2.31 (s, 3H, C*H*$_3$), 3.81 (s, 3H, OC*H*$_3$), 6.84 (m, 2H, ar C*H*), 7.13 (s, 1H, thienyl-C*H*), 7.28 (m, 1H, ar C*H*), 7.35 (m, 2H, ar C*H*), 7.44 (m, 2H, ar C*H*), 7.73 (m, 2H, ar C*H*); ^{13}C NMR ($CDCl_3$): δ 14.8, 55.8, 114.4, 122.6, 124.4, 125.8, 128.1, 128.2, 129.2, 132.0, 133.3, 142.8, 143.0, 165.2, 186.9; MS (CI): 483 (M^+).

Synthesis of DCTE Compounds ***7a–10a***: A solution of aldehyde **3** or the appropriate ketone **4–6** (0.1 mmol) and malonodinitrile (16.5 mg, 0.25 mmol) in anhydrous dichloroethane (5 mL) was cooled in an ice bath to 0 °C under nitrogen atmosphere and treated with $TiCl_4$ (0.1 mL, 0.91 mmol) dropwise. After stirring for 5 min, pyridine (0.2 mL) was carefully added over 20 min. The purple reaction mixture was allowed to warm to room temperature and subsequently heated at reflux for 5–10 min during which time a white precipitate formed and the color changed to pale brown. After cooling to room temperature, the solvents were evaporated under reduced pressure. The solid residue was dissolved in 15 % aqueous HCl (10 mL), the solution was extracted with chloroform (3 × 20 mL) and the combined organic layers were dried over $MgSO_4$, filtered and concentrated in vacuum. Purification of the crude product affords DCTE **7a–10a**.

7a was prepared from aldehyde **3** in 93 % yield (40 mg) as an orange solid. ^{1}H NMR spectroscopy indicated the product was pure enough to use without further purification. Mp = 102–104 °C; ^{1}H NMR ($CDCl_3$): δ 2.40 (s, 3H, C*H*$_3$), 7.18, 7.21 (2s, 2 × 1H, thienyl-C*H*, C=C*H*), 7.36 (m, 1H, ar C*H*), 7.42 (m, 2H, ar C*H*), 7.55 (m, 2H, ar C*H*); ^{13}C NMR ($CDCl_3$): δ 15.3, 92.6, 109.9, 112.6, 122.3, 124.4, 126.2, 129.0, 129.4, 132.5, 144.8, 145.3; ^{19}F NMR ($CDCl_3$): δ = –108.55, –113.49, –133.51; MS (CI): 425 (M^+); Anal Calcd. C 56.61, H 2.38, N 6.60; Found: C 56.32, H 2.50, N 6.77.

8a was prepared from ketone **4** and purified by column chromatography (SiO_2, hexane/ethyl acetate 10:1) on a short silica plug (2.5 cm ∅ × 4 cm) as an orange–yellow oil in 83 % yield (39 mg). ^{1}H NMR ($CDCl_3$): δ 1.03 (t, J = 7.0 Hz, 3H, C*H*$_3$), 1.66 (tq, J = 7.0, 7.0 Hz, 2H, C*H*$_2$), 2.45 (s, 3H, C*H*$_3$), 2.70 (m, 2H, C(O)C*H*$_2$), 7.03 (s, 1H, thienyl-C*H*), 7.34 (m, 1H, ar C*H*), 7.41 (m, 2H, ar C*H*), 7.52 (m, 2H, ar C*H*); ^{13}C NMR ($CDCl_3$): δ 14.2, 15.2, 21.7, 38.3, 93.0, 110.7, 123.2, 122.8, 126.0, 128.6, 129.4, 132.9, 142.6, 143.8, 167.4; ^{19}F NMR ($CDCl_3$): δ –110.02, –113.37, –134.36; MS (CI): 467 (M^+); Anal Calcd. C 59.22, H 3.46, N 6.01; Found: C 59.08, H 3.63, N 6.20.

9a was prepared from ketone **5** and purified by column chromatography (SiO_2, hexane/ethyl acetate 10:1) as an yellow solid in 74 % (39 mg). Mp = 110–111 °C; ^{1}H NMR ($CDCl_3$): δ 2.43 (s, 3H, C*H*$_3$), 6.88 (s, 1H, thienyl-C*H*), 7.32 (m, 1H, ar C*H*), 7.37 (m, 2H, ar C*H*), 7.41 (m, 2H, ar C*H*), 7.55 (m, 2H, ar C*H*), 7.63 (m, 3H, ar C*H*); ^{13}C NMR ($CDCl_3$): δ 15.1, 88.8, 111.9, 112.1, 122.5, 123.3, 125.9, 128.5, 129.3, 129.4, 129.8, 132.1, 132.9, 134. 2, 143.2, 143.5, 161.2; ^{19}F NMR ($CDCl_3$): δ <m->109.53, –113.52, –134.72; MS (CI): 501 (M^+); Anal Calcd. C 62.40, H 2.82, N 5.60; Found: C 62.16, H 3.01, N 5.30.

10a was prepared from ketone **6** and purified by column chromatography (SiO_2, hexane/ethyl acetate 10:1) as an orange oil in 36 % yield (19 mg). ^{1}H NMR ($CDCl_3$): δ 2.45 (s, 3H, C*H*$_3$), 3.89 (s, 3H, OC*H*$_3$), 6.87 (s, 1H, thienyl-C*H*), 7.02 (m, 2H, ar C*H*), 7.29 (m, 1H, ar C*H*), 7.36 (m, 4H, ar C*H*), 7.70 (m, 2H, ar C*H*); ^{13}C NMR ($CDCl_3$): δ 15.3, 56.1, 84.5, 112.6, 113.0, 114.8, 115.3, 122.7, 123.2, 124.0, 125.9, 128.4, 129.3, 129.9, 132.2, 133.0, 143.1, 143.2, 159.5, 164.9; ^{19}F NMR ($CDCl_3$): δ –110.13, –113.37, –134.79; MS (CI): 531 (M^+); Anal Calcd. C 61.13, H 3.04, N 5.28; Found: C 61.34, H 3.02, N 5.10.

Received: March 3, 2005
Final version: April 27, 2005
Published online: July 18, 2005

[1] a) S. Di Bella, *Chem. Soc. Rev.* **2001**, *30*, 355. b) T. Verbiest, S. Houbrechts, M. Kauranen, K. Clays, A. Persoons, *J. Mater. Chem.* **1997**, *7*, 2175.
[2] I. Asselberghs, K. Clays, A. Persoons, M. D. Ward, J. McCleverty, *J. Mater. Chem.* **2004**, *14*, 2831.
[3] a) M. Irie, in *Molecular Switches* (Ed: B. L. Feringa), Wiley-VCH, Weinheim, Germany **2001**, pp. 37–60. b) *Organic Photochromic and Thermochromic Compounds*, Vol. 1 (Eds: J. C. Crano, R. J. Guglielmetti), Plenum Press, New York **1999**, pp. 207–222.
[4] a) H. Tian, S. Yang, *Chem. Soc. Rev.* **2004**, *33*, 85. b) A. J. Myles, N. R. Branda, *Adv. Funct. Mater.* **2002**, *12*, 167. c) Special issue on *Photochromism: Memories and Switches* (Ed. M. Irie), *Chem. Rev.* **2000**, *100*.
[5] a) J. A. Delaire, K. Nakatani, *Chem. Rev.* **2000**, *100*, 1817. b) S. L. Gilat, S. H. Kawai, J.-M. Lehn, *Chem. Eur. J.* **1995**, *1*, 275. c) C. Bertarelli, A. Bianco, F. D'Amore, M. C. Gallazzi, G. Zerbi, *Adv. Funct. Mater.* **2004**, *14*, 357. d) J. M. Endtner, F. Effenberger, A. Hartschuh, H. Port, *J. Am. Chem. Soc.* **2000**, *122*, 3037.
[6] S. M. Shrestha, H. Nagashima, Y. Yokoyama, Y. Yokoyama, *Bull. Chem. Soc. Jpn.* **2003**, *76*, 363.
[7] A. Peters, C. Vitols, R. McDonald, N. R. Branda, *Org. Lett.* **2003**, *5*, 1183.
[8] Standard lamps used for visualizing thin-layer chromatography plates (Spectroline E-series, 470 μW cm^{-2}) were used to carry out the ring-closing reaction of all compounds. The ring-opening reactions were carried out using the light of a 150 W tungsten source that was passed through a 490 nm cut-off filter to eliminate higher-energy light.
[9] Semi-empirical calculations (AM1) using Spartan '02 from Wavefuntion, Inc., Irvine, CA were used for all estimations.
[10] a) A. Gazit, P. Yaih, C. Gilon, A. Levitzki, *J. Med. Chem.* **1989**, *32*, 2344. b) H. Hori, H. Nagasawa, M. Ishibashi, Y. Uto, A. Hirata, K. Sajijo, K. Ohkura, K. L. Kirk, Y. Uehara, *Bioorg. Med. Chem.* **2002**, *10*, 3257. c) A. Levitzki, *FASEB J.* **1992**, *6*, 3275.

A Method for the Rapid Synthesis of Large Quantities of Metal Oxide Nanowires at Low Temperatures**

By *Miran Mozetič*, *Uroš Cvelbar*, *Mahendra K. Sunkara*,* and *Sreeram Vaddiraju*

The utilization of metal oxide nanoparticles for refractive-index engineering in optical applications has recently been demonstrated.[1] To realize similar applications using nanowires, gram quantities are required. Hence, the large-scale

[*] Dr. M. K. Sunkara, S. Vaddiraju
Department of Chemical Engineering, University of Louisville
Louisville, KY 40292 (USA)
E-mail: mahendra@louisville.edu
Dr. M. Mozetič, U. Cvelbar
Plasma Laboratory F4, Jozef Stefan Institute
Jamova 39, Ljubljana SI-1000 (Slovenia)

[**] Supporting Information is available online from Wiley InterScience or from the author.

  DOI: 10.1002/adma.200500728

synthesis of nanowires in bulk quantities is essential not only to study the properties of these materials on the nanoscale,[2,3] but also for their use in various applications, such as composites, dispersions, catalysis, and biomedical engineering. Predominantly, nanowires are synthesized using catalyst clusters in either the vapor phase,[4,5] in a supercritical-fluid phase,[6] or by using an oxide-assisted growth technique without catalyst clusters.[7] Another prominent method employed is the bulk nucleation and growth of nanowires from the melts of low-melting-point metals.[8] The major drawback of these techniques is a slow growth rate—often on the order of a milligram per day. There have been some attempts to synthesize metal oxide nanowires by directly heating metal foils[9] or filaments[10] in an oxygen atmosphere, or by the chemical vapor transport of metal oxide species,[11,12] but the synthesis of nanowires using those methods requires relatively high temperatures. In order to overcome these limitations, we invented a method for the rapid synthesis of metal oxide nanowires directly from the solid phase at low temperatures (~ 50–300 °C). Our approach is based upon the control of growth parameters by exposing metal foils to low-pressure, weakly ionized, fully dissociated, and cold oxygen plasma. A plasma is an excited gas state often obtained by passing electrical current through a gas. The gaseous molecules are rapidly ionized, dissociated, and excited by inelastic collisions with electrons, and the properties of the gas are changed dramatically. At room temperature, the internal energy of gaseous particles (i.e., the average energy of the excited state) easily reaches several electron volts (eV). The internal energy may be high enough to completely dissociate oxygen molecules. Materials facing such plasmas are therefore exposed to an extremely large flux of neutral oxygen atoms, often exceeding 10^{24} m^{-2} s^{-1}.[13] Oxygen atoms are extremely reactive and oxidize practically all materials. Since there is often no potential energy barrier, the oxidation mechanism in plasmas is completely different from classical oxidation.

A niobium (Nb) foil, 0.015 mm thick, was exposed to an oxygen plasma for 90 s. Plasma parameters were measured with Langmuir and catalytic probes[14] and were as follows: the electron temperature was about 60 000 K, the ion density about 2×10^{16} m^{-3}, and the neutral oxygen atom density 6×10^{21} m^{-3}. The electron temperature was about 5 eV, as estimated from double electrical probe measurements. The surface of the sample after plasma treatment was observed using scanning electron microscopy (SEM). The SEM images reveal interesting structures. The entire surface of the niobium foil is covered with bundles of nanowires with submillimeter lengths, as shown in Figure 1a. The bundles consist of hundreds of well-oriented nanowires with cylindrical structures and similar, if not equal, diameters (Fig. 1b). The typical diameter of the nanowires is about 50 nm (Figs. 1b,c). The composition and phase of the nanowires were determined using Raman spectroscopy and transmission electron microscopy (TEM).

Chemical analysis of the bulk of the synthesized nanowires using Raman spectroscopy (Fig. 2) shows all peaks corresponding to Nb_2O_5, indicating that the nanowires are, in fact, composed of Nb_2O_5. A low-magnification TEM image of an as-synthesized Nb_2O_5 nanowire is presented in Figure 3a. The high-magnification TEM image in Figure 3b shows that no amorphous sheath surrounds the nanowire. The selected-area diffraction (SAD) pattern of the nanowires presented in the inset of Figure 3b clearly shows that the nanowire is monocrystalline Nb_2O_5 with a growth direction of [210].

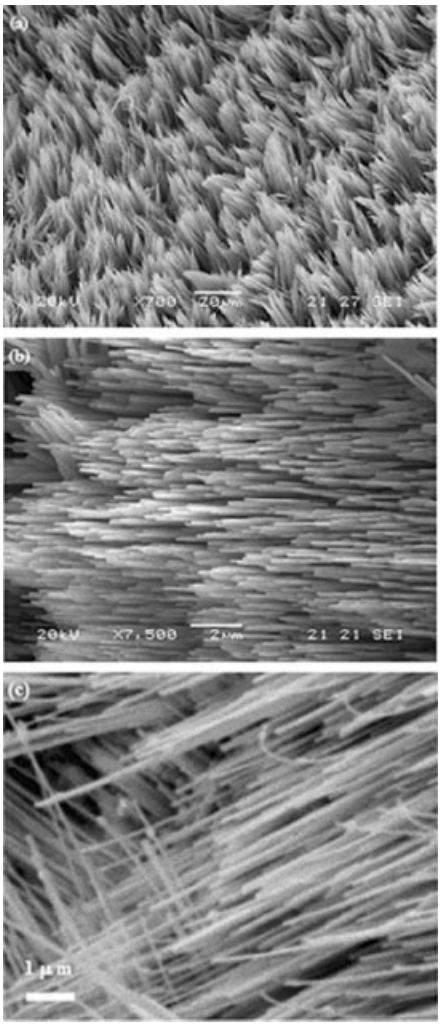

Figure 1. SEM images of Nb_2O_5 nanowires grown on Nb foil during plasma treatment at a high neutral O atom density. a) Low-magnification image of the nanowires and nanowire bundles. b) High-magnification image of a bundle of nanowires. c) High-magnification image of individual nanowires, with diameters of ~ 50 nm.

Experiments were also performed in which Nb foils were exposed to oxygen plasmas with varying densities of neutral oxygen atoms, while all other plasma parameters (such as the electron temperature, the ion density, and treatment time) remained the same. A couple of samples were exposed to plasma with an O density of 1.5×10^{21} m^{-3}. In this case, the O density was four times lower than that used in the previous experiments shown in Figures 1–3. The surface of such foils ap-

ADVANCED MATERIALS

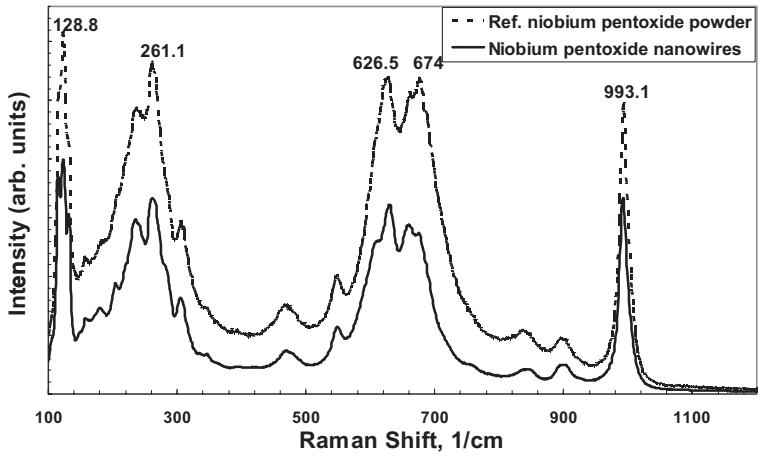

Figure 2. Raman spectrum of the synthesized Nb_2O_5 nanowires on bulk Nb foil using an oxygen plasma. The spectrum is identical to that obtained from commercially available Nb_2O_5 powder (also shown, Alfa Aesar, USA).

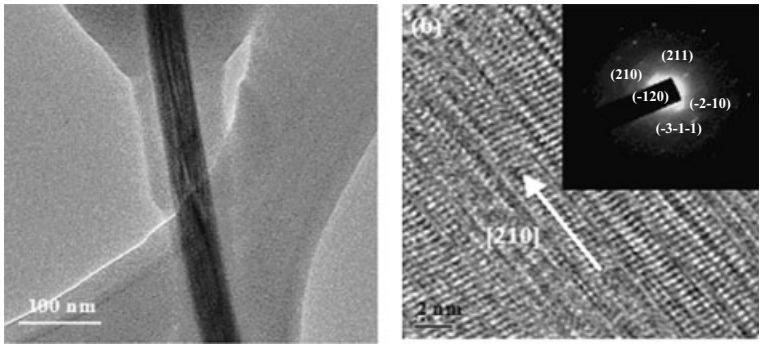

Figure 3. TEM analysis of a Nb_2O_5 nanowire synthesized by exposing Nb foil to a plasma composed of a high density of neutral oxygen (O) atoms. a) Low-magnification image. b) High-magnification TEM image of a Nb_2O_5 nanowire, showing no amorphous sheath on the surface. The selected-area diffraction pattern in the inset shows the growth direction to be [210].

pears rather free of nanowires; a detailed view of the surface, however, reveals some interesting features. The formation of thick Nb_2O_5 crystal nuclei along with the initial stages of growth of nanowires was observed (see Supporting Information). More samples were exposed to oxygen plasmas with O concentrations below 1×10^{21} m^{-3}. Under these conditions, no traces of any nanowires were observed, and the surface remained flat even after prolonged plasma treatment (see Supporting Information).

When a metal surface is exposed to a weakly ionized, fully dissociated oxygen plasma, it is exposed to a flux of plasma radicals, positive ions, and atoms. The electrons generated generally cause few surface effects. But, the electron–molecular collisions produce a certain amount of plasma radicals, such as O_2^+, O_2^-, O_2^*, O_2^v, O, O^+, O^-, O*, O_3, etc.

Plasma radicals interact with solid surfaces both physically and chemically. Positive ions are accelerated in the sheath between the plasma and the substrate (in our case the foil is at a floating potential of about 20 V). Assuming collisionless sheath approximation, ions are accelerated up to 20 eV just before reaching the surface. Ions are neutralized on the surface and transfer the major part of their kinetic and potential energies to the substrate. Since the energy is low, the sputtering of metal is negligible. However, the ions cause local distortion of the surface, as the excess energy displaces atoms around the collision spot. Yet, the flux of ions under our experimental conditions is low. The measured value of ion density in the plasma is about 2×10^{16} m^{-3} (measured with a double electrical probe). In inductively coupled plasmas at 27 MHz, the ions are perfectly thermalized, and their kinetic energy of random motion is below 0.1 eV. Therefore, the flux of ions onto the surface is approximately 4×10^{18} m^{-2} s^{-1}. Hence, if ions are primarily responsible for Nb oxidation, it would take several seconds just to form one monolayer (note that in the solid material there are approximately 10^{19} atoms m^{-2}). Since, the plasma treatment time in our experiment is about 90 s, ions would cause the formation of about a 10 nm thick layer only. This is far less than the measured lengths of the metal oxide nanowires. Positively charged oxygen ions are therefore not responsible for the growth of nanowires. In addition, negatively charged ions cannot reach the surface due to the sheath potential and are not believed to be responsible for the formation of nanowires.

The vibrational population of oxygen molecules in inductively coupled radio frequency (RF) plasmas is poor. This is due to very good coupling between vibrational and translational states in oxygen (the situation is completely different in nitrogen). The interaction of vibrationally excited molecules with solid materials is therefore always neglected.

Even though metastable oxygen molecules are likely to be produced in oxygen plasmas and to be stable in vacuum (de-excitation time by photon emission is of the order of a second), they have excitation energies around 1–2 eV, approximately. They are, however, likely to be relaxed on the surfaces of the discharge chamber. So, a typical density of O_2^* in inductively coupled plasmas is only of the order of 10^{17}–10^{18} m^{-3}. It is much lower than the density of neutral oxygen atoms.

Hence, the dominating O density should be responsible for rapid Nb oxidation. Most of the neutral oxygen atoms are in the ground state since the excited states are rapidly relaxed by photon emission. They are extensively produced by electron-impact dissociation and are stable and reactive in vacuum. The neutral oxygen (O) atom density in an oxygen plasma is largely dependent on the materials facing the plasma and is less likely to be dependent on electron density and electron temperature. (The recombination coefficient for the surface reaction $O + O \rightarrow O_2$ depends largely on the type of material as well as its roughness.) The electron temperature and/or density are im-

portant only because the O density depends on these two parameters. Generally, the degree of dissociation in oxygen plasmas can be anywhere between 10^{-6} and 1. In our case, we used smooth borosilicate glass with a recombination coefficient as low as about 10^{-4}. This allows for extremely high dissociation fractions. Under our experimental conditions, the O density is extremely high and is about 6×10^{21} m^{-3}. Hence, the O flux onto the Nb foil is of the order of 10^{24} $m^{-2}\,s^{-1}$. If all O atoms react, the oxide growth rate would be 10^5 monolayers per second. A foil of 15 μm thick consists of approximately 10^5 monolayers. So, if all atoms react, the foil should be fully oxidized in one second. In our experiential setup, the majority of the foil is oxidized within 90 seconds, which leads to the conclusion that the probability that an atom oxidizes the foil is of the order of 10^{-2}.

Experiments performed under various plasma conditions also indicated that the most important parameter was the density of neutral oxygen atoms in the plasma for oxide nanowire growth from Nb metal foil. We found that the Nb_2O_5 nanowires grew only when the neutral oxygen atom concentration exceeded about 2×10^{21} m^{-3}. Therefore, the nanowire production rate is limited by only two factors, namely, O density (or O flux onto the surface) and the size of the sample.

However, the observed growth of oxide crystals in one dimension directly from foils to form nanowires under high O radical flux conditions still requires an explanation. To this aim, we hypothesize a mechanism for the nucleation and growth of nanowires (see the schematic in Fig. 4). The supersaturation of subsurface depths of the Nb foil with oxygen (due to the interaction of the metal foil with the high flux of neutral oxygen atoms), the absence of Nb sputtering, and the limited Nb mobility at low temperatures are used as critical steps to explain the observed metal oxide nanowire growth. The steps involved in the formation of Nb_2O_5 nanowires from Nb foils at low temperatures are as follows:

1) Diffusion and dissolution of atomic oxygen from the gas phase into the niobium metal (Fig. 4a).

2) Nucleation of niobium oxide on the surface, due to the supersaturation of the surface with oxygen (Fig. 4b).

3) Growth of niobium oxide nanowires from the bottom (basal growth) because of the constant supply of oxygen into the niobium metal. (Fig. 4c). Here, niobium is supplied only from the metal at the bottom, (since this process occurs at low temperature, there is no metal in the vapor phase) and oxygen is supplied from the vapor phase. This allows for the growth of niobium oxide only in the form of nanowires since niobium has a limited mobility at low temperature (~50–300 °C), and the niobium oxide formed has to attach at the base of the nuclei formed.

Previously, we reported the synthesis of low-melting-point metal oxide nanowires by the direct dissolution of oxygen into molten-metal pools.[15] Since the solubility of oxygen in these metals is extremely low, supersaturation of the metal with oxygen led to the multiple nucleation and growth of nanowires from molten-metal droplets. The exposure to O_2/H_2 plasma at modest temperatures (400–500 °C) typically led to bulk saturation of molten metals and the nucleated crystals grew vertically, with basal attachment, into one-dimensional (1D) structures. However, in this work, the dissolution of oxygen into niobium should lead to supersaturation of only the subsurface and not the entire bulk of the metal foil due to the low temperatures, short duration of exposure, and high flux of O atoms. The supersaturation of the Nb subsurface layers due to the influx of atomic oxygen leads to spontaneous nucleation of nanometer-scale Nb_2O_5 crystals. The limited mobility of Nb at low temperatures makes the nuclei grow vertically by means of the basal attachment of Nb and O, similar to our earlier experiments with molten metals.

In addition, plasma-oxidation experiments using vanadium foils also resulted in the growth of vanadium pentoxide nanowires directly from the vanadium foils (see Supporting Information). These results with vanadium foils suggest that this technique should work for other metals as well, such as tantalum and iron. However, the oxygen-atom-density window is expected to differ from one material to the next. It is possible to use thin metal films attached onto foreign substrates instead of foils. In addition to oxides, we believe that this nanowire synthesis method has widespread applicability to the synthesis of other compound systems, such as nitrides, sulfides, phosphides, and arsenides. Much of this work is an on-going study, and the results will be published in the future.

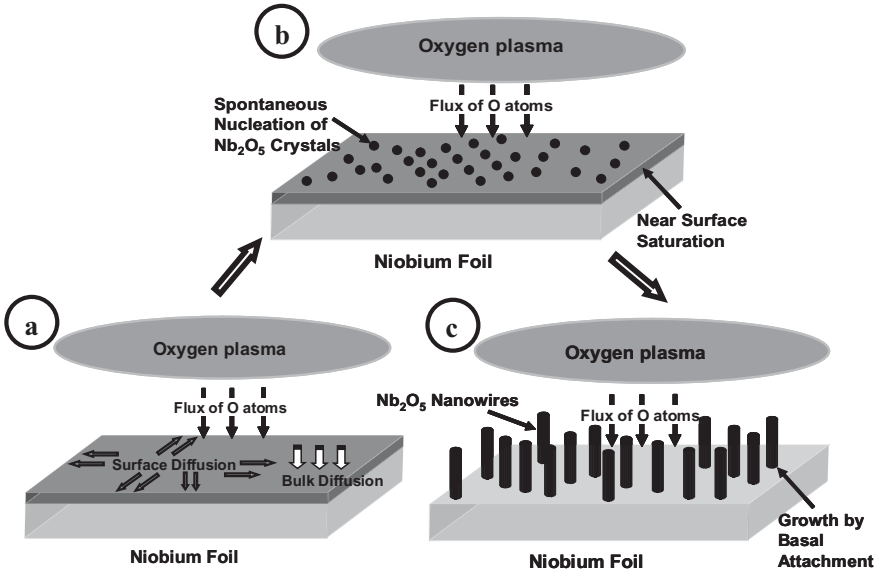

Figure 4. Schematic representation of the growth mechanism involved in the formation of metal oxide nanowires from bulk material when exposed to a highly dissociated oxygen plasma. a) Diffusion and dissolution of oxygen from the gas phase into the bulk Nb metal. b) Nucleation of Nb_2O_5 on the surface of Nb due to the supersaturation of the metal surface with oxygen. c) Growth of Nb_2O_5 nuclei into nanowires due to the basal attachment of Nb and O to the nuclei (basal growth).

ADVANCED MATERIALS

Nb_2O_5 nanowires by themselves may find interest in future field-emission displays[16] as well as in microelectronics. Unlike other synthesis methods where nanomaterials take a long time to grow, Nb_2O_5 and other metal oxide nanowires produced via the cold plasma treatment using a high neutral O flux described here grew rather rapidly. Under our experimental conditions, the entire foil (20 mm × 4 mm) was covered with nanowires in just 90 s. The fast growth rates obtained for nanowire growth combined with low-temperature operation allows us to visualize a possible semibatch- and batch-type manufacturing technique for large quantities of nanowires.

Experimental

Nanowires were synthesized directly from the solid state by the exposure of Nb foil to oxygen plasma. High purity Nb foil 0.15 mm thick was cut into rectangular pieces approximately 20 mm × 4 mm and exposed to a highly dissociated, weakly ionized oxygen plasma created in an inductively coupled high RF discharge. The experiments were performed in a vacuum system pumped with a two-stage oil rotary pump with an ultimate pressure of about 0.1 Pa. A schematic of the setup used for the synthesis of the nanowires is shown in Figure 5. After evacuating the chamber to the base pressure, commercially available oxygen was continuously leaked into the system. The chamber was maintained at a pressure of 100 Pa during the experiments. The plasma

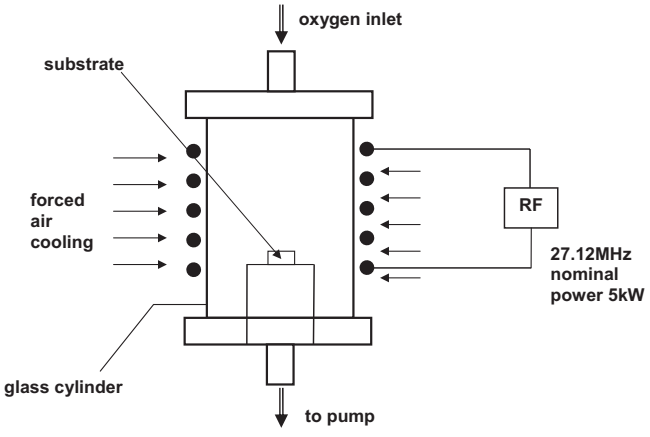

Figure 5. Schematic representation of the experimental setup used for the synthesis of metal oxide nanowires.

was created by an inductively coupled RF generator with a maximum power of 5 kW. The power used during the experiments was about 1.5 kW. Plasma characteristics were measured using Langmuir and catalytic probes. The typical plasma discharge characteristics during the experiments were as follows: the electron temperature was about 5 eV, the ion density was about 2×10^{16} m^{-3}, and the neutral oxygen atom density was in the range of 1×10^{21}–6×10^{21} m^{-3}. The foil samples were left in the plasma for 90 s. After the plasma treatment, the samples were characterized using scanning electron microscopy (SEM), Raman spectroscopy, and transmission electron microscopy (TEM).

Received: April 10, 2005
Final version: May 4, 2005
Published online: July 26, 2005

[1] K. Krogman, T. Druffel, M. K. Sunkara, *Nanotechnology* **2005**, *16*, 338.
[2] A. P. Alivisatos, *Science* **1996**, *271*, 933.
[3] A. M. Saitta, F. Buda, G. Fiumara, P. V. Giaquinta, *Phys. Rev. B* **1996**, *53*, 1446.
[4] R. M. Wagner, W. C. Ellis, *Appl. Phys. Lett.* **1964**, *4*, 89.
[5] A. M. Morales, C. M. Lieber, *Science* **1998**, *279*, 208.
[6] J. D. Holmes, K. P. Johnston, R. C. Boty, B. A. Korgel, *Science* **2000**, *287*, 1471.
[7] Y. H. Tang, Y. F. Zhang, H. Y. Peng, N. Wang, C. S. Lee, S. T. Lee, *Chem. Phys. Lett.* **1999**, *314*, 16.
[8] M. K. Sunkara, S. Sharma, R. Miranda, G. Lian, E. C. Dickey, *Appl. Phys. Lett.* **2001**, *79*, 1546.
[9] Y. Q. Jhu, W. Hu, W. K. Hsu, M. Terrones, N. Grobert, J. P. Hare, H. W. Kroto, D. R. M. Walton, H. Terrones, *Chem. Phys. Lett.* **1999**, *309*, 327.
[10] G. Gu, B. Zheng, W. Q. Han, S. Roth, J. Liu, *Nano Lett.* **2002**, *2*, 849.
[11] J. G. Liu, Y. Zhou, Z. Y. Zhang, *J. Phys. Condens. Matter* **2003**, *15*, L453.
[12] S. Vaddiraju, H. Chandrasekaran, M. K. Sunkara, *J. Am. Chem. Soc.* **2003**, *125*, 10 792.
[13] M. Mozetič, A. Ricard, D. Babic, I. Poberaj, J. Levaton, V. Monna, U. Cvelbar, *J. Vac. Sci. Technol. A* **2003**, *21*, 369.
[14] D. Babic, I. Poberaj, M. Mozetič, *Rev. Sci. Instrum.* **2001**, *72*, 4110.
[15] S. Sharma, M. K. Sunkara, *J. Am. Chem. Soc.* **2002**, *124*, 12 288.
[16] M. Žumer, V. Nemanic, B. Zajec, M. Remškar, A. Mrzel, D. Milhailovic, *Appl. Phys. Lett.* **2004**, *84*, 3615.

Energetic Ionic Liquids from Azido Derivatives of 1,2,4-Triazole**

By *Hong Xue* and *Jean'ne M. Shreeve**

In recent years, the synthesis of energetic heterocyclic compounds has attracted considerable interest.[1–5] Modern energetic materials derive most of their energy either from oxidation of the carbon backbone, as traditionally found for energetic materials, or from their high, positive heats of formation.[6,7] Recently, the syntheses of new members of heterocyclic-based energetic, low-melting salts have been described.[8,9] Energetic materials that are salts often possess advantages over non-ionic molecules since these moieties tend to exhibit lower vapor pressure and higher densities than their atomically similar non-ionic analogues. In these ionic species, the cation is generally a bulky organic ion with low symmetry.

[*] Prof. J. M. Shreeve, Dr. H. Xue
Department of Chemistry, University of Idaho
Moscow, ID 83843-2343 (USA)
E-mail: jshreeve@uidaho.edu

[**] The authors gratefully acknowledge the support of AFOSR (F49620-03-1-0209), NSF (CHE0315275), and ONR (N00014-02-1-0600). We are grateful to Dr. Gary Knerr and Dr. Alex Blumenfeld for mass spectra and NMR analyses, respectively.

  DOI: 10.1002/adma.200500789